Stem Cell Reports
Report
ISSCR
OPEN ACCESS

Genetic variation modulates susceptibility to aberrant DNA hypomethylation and imprint deregulation in naive pluripotent stem cells

C. Parikh,[1,2,11] R.A. Glenn,[3,4,5,11] Y. Shi,[6,11] K. Chatterjee,[1] K. Kasliwal,[1] E.E. Swanzey,[7] S. Singer,[3,4] S.C. Do,[3,4] Y. Zhan,[9] Y. Furuta,[9] M. Tahiliani,[10] E. Apostolou,[1] A. Polyzos,[1] R. Koche,[8] J.G. Mezey,[6,*] T. Vierbuchen,[3,4,*] and M. Stadtfeld[1,12,*]

[1]Sanford I. Weill Department of Medicine, Sandra and Edward Meyer Cancer Center, Weill Cornell Medicine, New York, NY 10065, USA
[2]Department of Molecular, Cell and Cancer Biology, University of Massachusetts Chan Medical School, Worcester, MA 01655, USA
[3]Developmental Biology Program, Sloan Kettering Institute, Memorial Sloan Kettering Cancer Center, New York, NY 10065, USA
[4]Center for Stem Cell Biology, Sloan Kettering Institute, Memorial Sloan Kettering Cancer Center, New York, NY 10065, USA
[5]Cell and Developmental Biology Program, Weill Cornell Graduate School of Medical Sciences, Cornell University, New York, NY, USA
[6]Department of Computational Biology, Cornell University, Ithaca, NY 14853, USA
[7]The Jackson Laboratory, Bar Harbor, ME 04609, USA
[8]Center for Epigenetics Research, Memorial Sloan Kettering Cancer Center, New York, NY 10065, USA
[9]Mouse Genetics Core Facility, Sloan Kettering Institute, Memorial Sloan Kettering Cancer Center, New York, NY 10065, USA
[10]Department of Biology, New York University, New York, NY 10003, USA
[11]These authors contributed equally
[12]Lead contact
*Correspondence: jgm45@cornell.edu (J.G.M.), vierbuct@mskcc.org (T.V.), mas4011@med.cornell.edu (M.S.)
https://doi.org/10.1016/j.stemcr.2025.102450

SUMMARY

Naive pluripotent stem cells (nPSCs) frequently undergo pathological loss of DNA methylation at imprinted gene loci, posing a hurdle for biomedical applications and underscoring the need to identify underlying causes. We show that nPSCs from inbred mouse strains exhibit strain-specific susceptibility to locus-specific deregulation of imprinting marks during reprogramming and upon exposure to a mitogen-activated protein kinase (MAPK) inhibitor, a common approach to maintain naive pluripotency. Analysis of genetically diverse nPSCs from the Diversity Outbred (DO) stock confirms the impact of genetic variation on epigenome stability, which we leverage to identify *trans*-acting quantitative trait loci (QTLs) that modulate DNA methylation levels at specific targets or genome-wide. Analysis of multi-target QTLs on chromosomes 4 and 17 suggests candidate transcriptional regulators contributing to DNA methylation maintenance in nPSCs. We propose that genetic variants represent biomarkers to identify pluripotent cell lines with desirable properties and may allow the targeted engineering of nPSCs with stable epigenomes.

INTRODUCTION

Naive pluripotent stem cells (nPSCs) are capable of extensive *ex vivo* self-renewal, amenable to lead genome engineering, and can differentiate into all somatic cell types. This combination of features makes nPSCs, in principle, tailor-made for regenerative medicine applications. However, the pervasive epigenetic instability of nPSCs upon *ex vivo* culture—which manifests as aberrant changes in DNA methylation and other chromatin marks that compromise physiological transcriptional programs and functional properties (Mani and Mainigi, 2018; Rebuzzini et al., 2016)—represents a significant roadblock for many biomedical applications of pluripotent stem cells (PSCs).

Aberrant DNA methylation changes in cultured nPSCs include hypermethylation and hypomethylation (Habibi et al., 2013; Lee et al., 2018) and affect gene loci encoding essential developmental regulators. Solidifying naive pluripotency by chemical inhibition of mitogen-activated protein kinase (MAPK) signaling, an approach often applied for both mouse and human cells, results in widespread loss of DNA methylation in both species. Epigenetic changes are particularly problematic at imprinted genes since the loss of the parent-of-origin asymmetry in DNA methylation at these loci cannot be readily restored (Bayerl et al., 2021; Pastor et al., 2016) and is associated with specific defects in embryonic development (Ferguson-Smith and Bourc'his, 2018) that complicate disease modeling with affected cells.

DNA methylation abnormalities in naive nPSCs are associated with a high degree of line-to-line variability, even when established under identical conditions (Bock et al., 2011; Humpherys et al., 2001; Johannesson et al., 2014). This has given rise to the notion that randomly occurring pathological epigenome changes in nPSCs are an unavoidable side effect of the extraordinary developmental flexibility of these cells. Several recent studies leveraging inbred mouse strains with fully sequenced genomes and high-resolution panels of single-nucleotide polymorphisms (SNPs) have shown that core PSC properties such as self-renewal capacity (Skelly et al., 2020) and *in vitro* differentiation bias (Byers et al., 2022; Ortmann et al., 2020) are modulated by genetic variation. In addition, pathological DNA hypermethylation at the *Dlk1-Dio3* locus in nPSCs is controlled

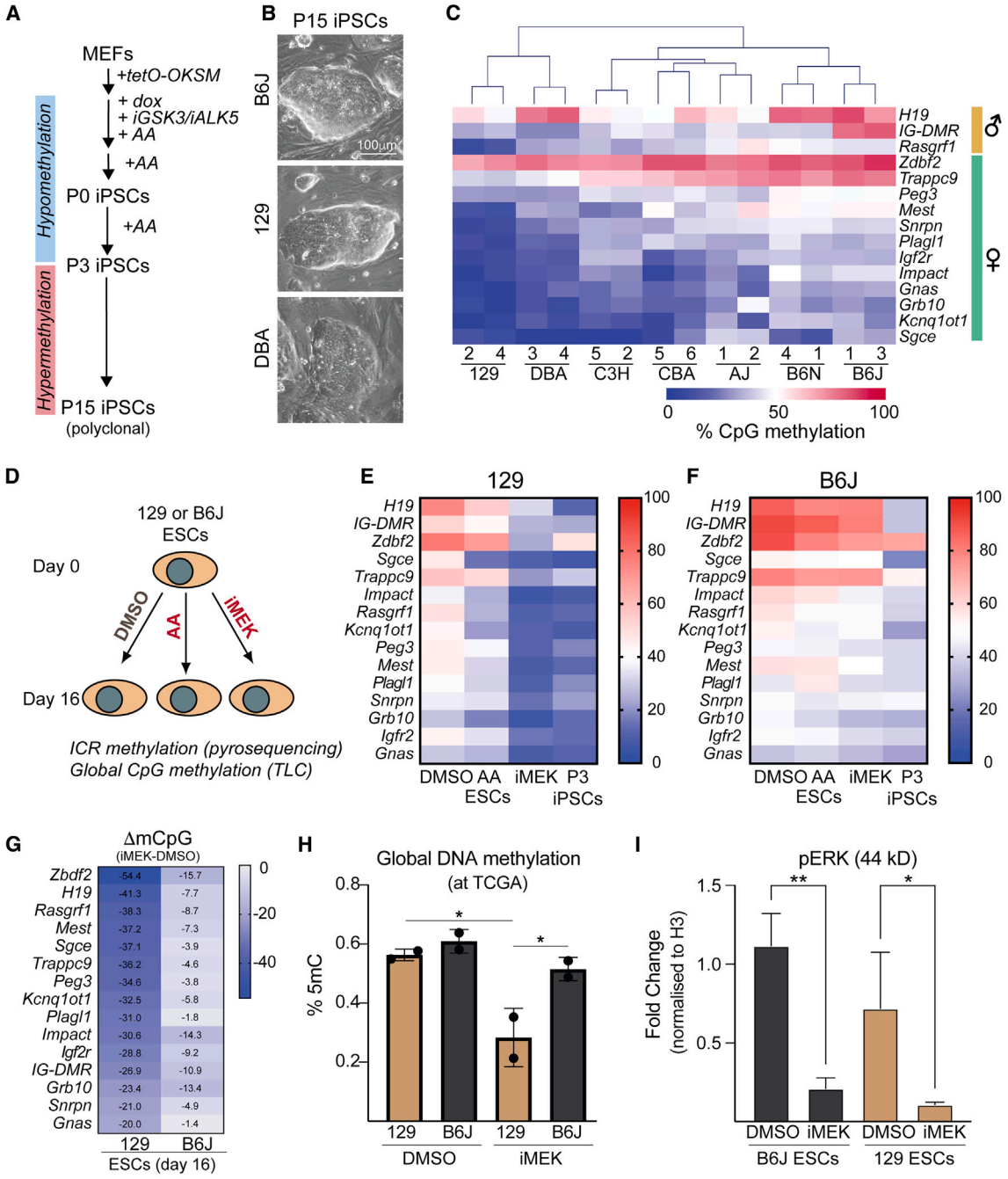

Figure 1. Genetic variation modulates DNA hypomethylation at ICRs in naive pluripotent stem cells from distinct inbred mouse strains

(A) Experimental strategy to derive polyclonal iPSCs from inbred strains.

(B) Representative colony morphology of P15 iPSCs.

(C) Unsupervised clustering of ICR methylation levels in polyclonal iPSCs (n = 2 independent cell lines/strain).

(D) Strategy to test the impact of AA or iMEK on imprint methylation in 129 and B6J mESCs. TLC, thin-layer chromatography.

(E) DNA methylation levels at ICRs in indicated cell types derived from the 129 strain.

(F) Same as (E) but for the B6J strain.

(G) Average changes in DNA methylation levels (iMEK minus DMSO) at ICRs in 129 and B6J ESCs.

(legend continued on next page)

by a *trans*-acting quantitative trait locus (QTL) that distinguishes the commonly used B6J and 129 strains (Swanzey et al., 2020). Whether this observation extends to other imprinted gene loci or the susceptibility of nPSCs for DNA hypomethylation remains unanswered.

Here, we use nPSCs from a combination of distinct inbred strains and a genetically diverse outbred stock to systematically characterize the impact of genetic variation on DNA methylation loss at imprinting control regions (ICRs). Our data indicate that susceptibility to DNA hypomethylation in nPSCs is determined by identifiable genetic variants. We reveal candidate regulators of DNA methylation levels via QTL mapping and suggest approaches to stabilizing the epigenome of nPSCs.

RESULTS

Strain-specific introduction of imprint abnormalities in iPSCs established from inbred mice

To investigate whether genetic background influences the stability of imprinting marks during nPSC derivation and maintenance, we used OCT4, KLF4, SOX2, and MYC (OKSM) reprogramming (Sommer et al., 2009) to establish induced PSCs (iPSCs) from mouse embryonic fibroblasts (MEFs) of seven inbred mouse strains (129S1/SVlmJ; 129, C57BL6/J; B6J, C57BL6/NJ; B6N, CBA/J; CBA, DBA/2J; DBA, C3H/HeJ; C3H, and A/J; AJ) (Figure S1A). We cultured cells undergoing reprogramming in media containing ascorbic acid (AA) and modulators of WNT and transforming growth factor β signaling (Figure 1A), which dramatically facilitates iPSC formation (Vidal et al., 2014). Since AA has been shown to stimulate TET enzymes (Blaschke et al., 2013), we reasoned that limited exposure to this compound might reveal strain-specific susceptibilities to DNA demethylation. In contrast, prolonged culture in standard serum-containing media (Figure 1A) would reveal susceptibilities to DNA hypermethylation. We focused on male cells to avoid confounding our results with the well-documented DNA hypomethylation propensity observed in female nPSCs (Zvetkova et al., 2005). We obtained stable iPSC colonies independent of transgenic OKSM expression from each of the seven inbred strains, including the CBA and DBA strains that are not permissive for embryonic stem cell (ESC) derivation in standard conditions (Czechanski et al., 2014), albeit at variable efficiencies (Figure S1B). Expanded polyclonal iPSC lines (n = 2 cell lines derived from independent MEF preps for each inbred strain; Table S1) exhibited the expected pluripotent cell morphology (Figure 1B) and expression of the pluripotency-associated markers SSEA1 and EpCAM (Figure S1C).

To assess the status of imprinted gene regulation, we subjected genomic DNA (gDNA) isolated from passage 15 (P15) iPSCs for DNA methylation analysis by targeted bisulfite sequencing, focusing on established control regions of the three paternally imprinted loci (*Dlk1-Dio3*, *H19/Igf2*, and *Rasgrf1*) and 12 maternally imprinted loci (*Gnas*, *Grb10*, *Igf2r*, *Impact*, *Inpp5f*, *Kcnq1ot1*, *Mest*, *Nap1l5*, *Nnat*, *Peg3*, *Plagl1*, *Sgce*, *Snrpn*, *Trappc9*, *Zdbf2*, and *Zrsr1*). Unsupervised clustering of these DNA methylation data revealed considerable locus-to-locus and strain-to-strain variability in DNA methylation levels. However, independent cell lines from each genetic background clustered together (Figure 1C), suggesting a significant contribution of genetic background to imprint stability. For further analyses, we defined hypermethylation as >70% CpG methylation and hypomethylation as <20% CpG methylation at a given locus based on average values from independent cell lines. With these criteria, hypermethylation of *Dlk1-Dio3* (controlled by the intergenic differentially methylated region, *IG-DMR*) was only observed in B6J-iPSCs, (Figure S1A), suggesting that the genetic variant(s) predisposing nPSCs to pathological DNA hypermethylation at this locus are uniquely present or active in B6J mice. Additional evidence that genetic background controls locus-specific DNA hypermethylation comes from analysis of *H19* (DBA-, B6N-, and B6J-iPSCs) and *Trappc9* (C3H-, CBA-, AJ-, B6N-, and B6J-iPSCs) (Figure 1C). In contrast, *Zdbf2* exhibited hypermethylation in iPSCs from all inbred strains (Figure 1C). Focusing on DNA hypomethylation, we observed multi-locus loss of imprint methylation in iPSCs from 129 (10 loci), DBA (7 loci), CBA (4 loci), and C3H (2 loci) (Figure 1C), indicating either the presence of multiple variants that affect individual genes or the existence of variants that affect DNA methylation at multiple loci.

To further investigate strain-specific susceptibilities to DNA methylation change and to determine when, during the iPSC derivation process, they might manifest, we focused on 129 and B6J, the two backgrounds with the most divergent DNA methylation profiles in P15 iPSCs (Figure 1C). While MEFs from 129 and B6J mice showed indistinguishable, physiological DNA methylation levels at all ICRs (Figure S1D), P3 129 iPSCs (methylation analysis concomitant with AA withdrawal; see Figure 1A) already exhibited pronounced DNA hypomethylation introduced during the reprogramming process. In contrast, DNA

(H) Global DNA methylation levels by thin-layer chromatography in indicated mESCs after 16 days of culture with either DMSO or of iMEK. *p < 0.05 with one-way ANOVA; n = 2 independent cell lines for each background and condition.

(I) Phosphorylated ERK protein levels in 129 and B6J mESCs after culture in iMEK or DMSO. Protein levels are normalized to histone H3 expression. *p < 0.05 and **p < 0.01 with one-way ANOVA; n = 3 independent cell lines for each background and condition.

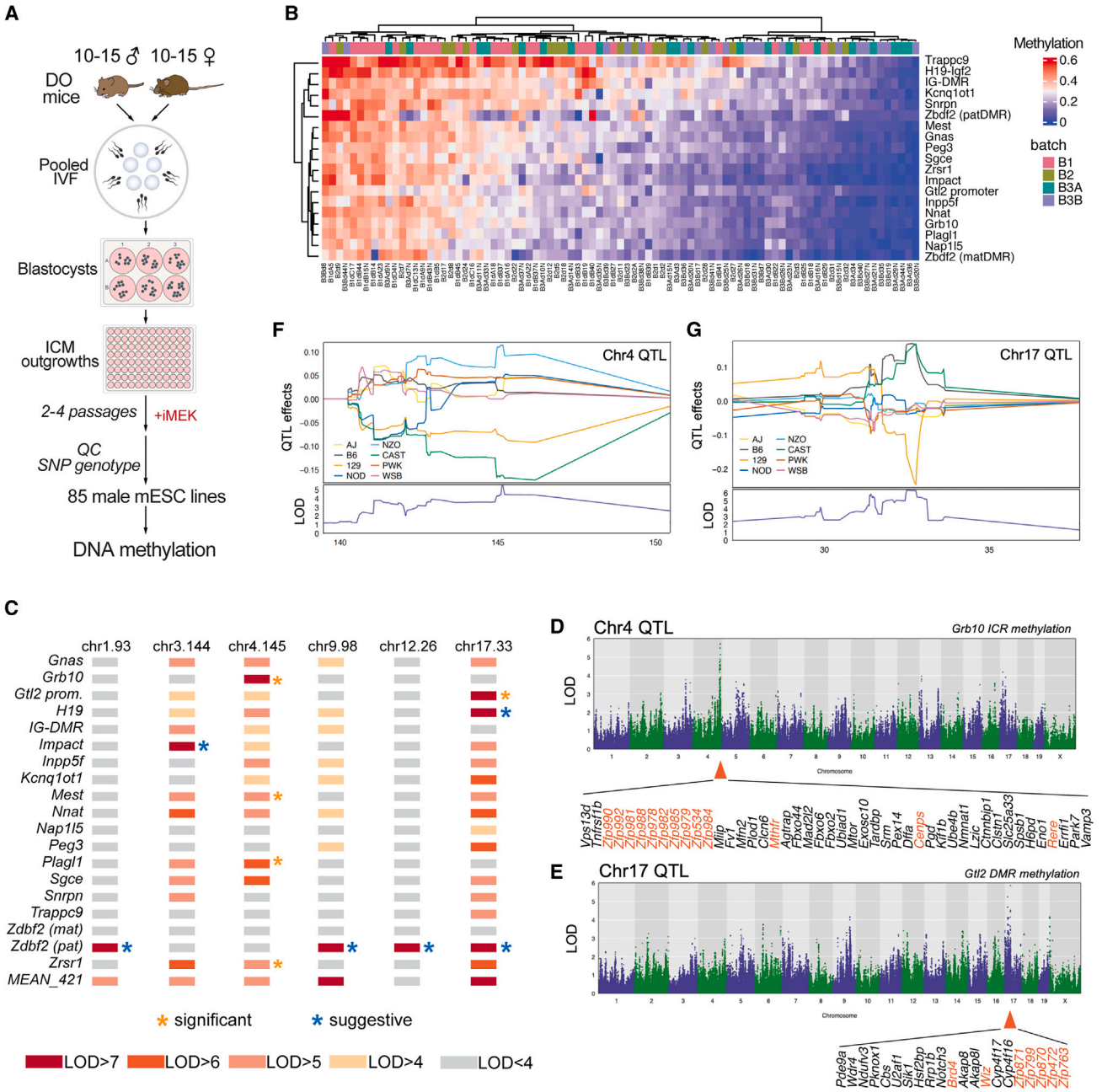

Figure 2. Identification of QTLs modulating pathological DNA hypomethylation at ICRs in naive PSCs

(A) DO mESCs were generated via a pooled *in vitro* fertilization approach. Male lines (n = 85) were banked at early passage (p3) and then thawed and cultured for an additional two passages in serum/LIF + 2i to promote hypomethylation of ICRs.

(B) ICR DNA methylation levels across DO mESC lines (n = 85).

(C) Genome-wide significant (FWER < 0.1) and suggestive (FWER < 0.2) QTLs controlling ICR methylation.

(D) Genome-wide LOD scores for methylation at the *Grb10* ICR. The red arrowhead indicates the Chr4 QTL. Genes with tpm > 10 in either B6J or 129 mESCs within the QTL region are listed, highlighting known transcriptional or chromatin regulators.

(E) Genome-wide LOD scores for methylation at the *Gtl2* promoter. The Chr17 QTL and encoded genes are highlighted.

(legend continued on next page)

hypermethylation was not evident at ICRs in B6J iPSCs at this earlier stage of derivation (Figure S1D), suggesting that DNA hypermethylation is introduced during prolonged culture in the absence of AA. Together, these observations reveal strain-specific differences in the stability of DNA methylation levels at imprinted gene control regions in iPSCs derived under identical conditions.

Susceptibility to DNA hypomethylation upon MAPK inhibition is governed by genetic background

To determine whether nPSCs derived using other standard approaches also exhibit strain-specific differences to loss-of-imprinting by DNA hypomethylation as observed in iPSCs, we exposed ESCs established from 129 and B6J blastocysts to either AA or the MAPK inhibitor PD0325901 ("iMEK") for 16 days (Figure 1D), resembling the time required to reprogram MEFs into early-stage iPSCs. 129 ESCs cultured in the presence of AA showed evidence for DNA hypomethylation, albeit significantly less severe than P3 iPSCs (Figures 1E and S1E), suggesting that reprogramming can exacerbate the loss of methylation at ICRs. In contrast, 129 ESCs exposed to iMEK showed a dramatic loss of ICR methylation at all loci studied, similar to what was observed in P3 iPSCs (Figure 1E). This is in agreement with the reported role of MEK inhibition in DNA demethylation (Choi et al., 2017; Yagi et al., 2017). Compared to 129 ESCs, B6J ESCs cultured with either AA or iMEK exhibited a modest reduction in ICR methylation, which remained in the physiological range (Figures 1F and S1E). This documents a surprising degree of resistance of B6J ESCs to pathological DNA hypomethylation that extends to all ICRs analyzed (Figure 1G). Of note, DNA methylation levels in F1 hybrid mouse ESCs (mESCs) exposed to iMEK were in between levels observed in pure background mESCs (Figure S1F), suggesting that the genetic factors involved in this phenotype function in an additive manner.

We conducted thin-layer chromatography experiments to determine whether loss of ICR methylation in 129 mESCs reflects genome-wide changes in total DNA methylation levels. This approach revealed significantly reduced global levels of DNA methylation at CpG residues in 129 mESCs but not in B6J exposed to iMEK. In contrast, mESCs from both strains cultured in standard conditions showed similar DNA methylation levels (Figure 1H). These observations suggest that the effects of genetic background on susceptibility to DNA hypomethylation downstream of MAPK inhibition are not restricted to ICRs, which is consistent with prior observations made in mouse and human nPSCs (Choi et al., 2017; Pastor et al., 2016). Of note, the reduction in ERK phosphorylation (Figure 1I) and the levels of DNMT3A (Figure S1G) were similar in 129 and B6J ESCs exposed to iMEK. These results demonstrate that the observed differences in DNA methylation stability between mESCs from these two strains are not due to the different effectiveness of the inhibitor. They also suggest that the responsible variants influence the recruitment or activity of DNA methyltransferases rather than directly altering the expression levels of these enzymes. Together, our findings demonstrate that susceptibility to pathological loss of DNA methylation in commonly used nPSC culture conditions is strongly modulated by genetic variation.

Variable DNA hypomethylation in naive PSCs derived from a genetically diverse outbred mouse stock

Our results so far document that genetic variation between nPSCs from different inbred mouse strains results in markedly different susceptibility to hypomethylation of ICRs driven by MAPK inhibition. We sought to determine whether a similar effect is evident in genetically diverse nPSCs that better model the high levels of genetic variation and heterozygosity in the human population and would allow the mapping of underlying variants. To this end, we used a pooled *in vitro* fertilization (IVF) approach to establish a large panel of genetically diverse ESC lines from Diversity Outbred (DO) mice (Glenn et al., 2024) (Figure 2A), a heterogeneous outbred stock derived from eight founder strains (AJ, B6J, 129, NOD/ShiLtJ; NOD, NZO/HlLtJ; NZO, CAST/EiJ; CAST, PWK/PhJ; PWK, and WSB/EiJ; WSB) that harbors more than 40 million SNPs and structural variants and allows high-resolution genetic mapping (Gatti et al., 2014; Swanzey et al., 2021). Pooled IVF was used to enable the scalable production of genetically diverse nPSC lines (see Glenn et al., 2024 for additional details of this approach). Kinship analysis of DO nPSC lines using SNP genotyping data demonstrated that a majority of the nPSC lines derived from this pooled IVF approach are from distinct sets of parents (i.e., non-siblings), which ensures that statistical power to map QTLs is not reduced due to a high degree of relatedness between nPSC lines used for QTL mapping (Figure S2A). For our experiments, we collected gDNA from a panel of 85 male DO mESC lines that exhibited undifferentiated morphology. These cells

(F) An allelic effect plot for the Chr4 QTL shows the relationship between the genotype (i.e., strain) at the QTL region and the observed effect on DNA methylation (upper). Of the eight possible strain haplotypes at this region, which can show distinct associations with the phenotype (*Grb10* ICR methylation), the NZO haplotype is correlated with higher levels of DNA methylation. In contrast, the CAST haplotype is associated with lower DNA methylation levels. The LOD score (lower) indicates the genomic location of the SNPs with the strongest statistical association with the phenotype.
(G) Allelic effect plot for the Chr17 QTL. Note that B6J and 129 haplotypes show opposite effects on DNA methylation levels.

were cultured in the presence of iMEK for 2–4 passages to promote hypomethylation (Figure 2A).

To sensitively measure DNA methylation levels at ICRs and at additional selected loci across the genome (Figure S2B; Table S2) in DO ESC lines, we used enzymatic methyl (EM)-seq and a custom targeted capture panel. Unbiased clustering of DNA methylation levels at all regions revealed markedly different DNA methylation levels across the panel of DO nPSC lines (Figure S2C). ICRs had the highest average levels of DNA methylation among the various categories of *cis*-regulatory elements included within the targeted capture panel (Figure S2D). Notably, differences in CpG methylation levels were not correlated with differences in sequencing coverage (Figure S2E), confirming the reliability of our approach. These data suggest that ICRs in nPSCs might have increased protection from demethylation compared to other gene loci, potentially reflecting their increased resistance to genome-wide epigenetic reprogramming in the preimplantation embryo. Nevertheless, DNA methylation levels at ICRs were also highly variable between DO cell lines, ranging from physiological levels (~50%) of DNA methylation at all ICRs in some cell lines to essentially complete loss of methylation at all ICRs in other lines (Figure 2B). These data suggest that genetic variation present within the DO stock can influence DNA hypomethylation phenotypes in naive PSCs cultured with iMEK.

To evaluate whether different ICRs respond similarly to MAPK inhibition, we performed principal component analysis on ICR DNA methylation data across the panel of DO nPSC lines. This analysis indicated that most ICRs respond in a strongly correlated manner (Figure S2F), except for (1) regions controlling imprinting at the two major paternally imprinted gene clusters (IG-DMR and *H19-Igf2*), (2) a somatic DMR at the maternally imprinted *Zdbf2* locus that acquires DNA methylation on the paternal allele late during embryogenesis (Duffié et al., 2014), and (3) *Trappc9*, a locus encoding transcripts known to exhibit variable patterns of parent-of-origin specific imprinting during brain development (Claxton et al., 2022). Consistent with our results with iPSCs from distinct inbred strains, these data provide extensive additional evidence that the majority of ICRs undergo pathological loss of DNA methylation in response to iMEK treatment and that genetic variation modulates the susceptibility of pathological hypomethylation in a similar manner across most ICRs. The observed differences in the relative susceptibility of a subset of ICRs might reflect distinct regulatory mechanisms operational at these sites during development.

Identification of QTLs determining susceptibility to locus-specific and widespread DNA hypomethylation

We leveraged the observed variation in DNA methylation levels at imprinted gene loci (Figure 2B) across DO nPSC lines to map QTLs for all ICRs (ICR-me QTLs) across 73 lines that passed additional quality control criteria (see methods). This resulted in the identification of six QTLs that reached statistical significance for at least one ICR (see methods) (Figure 2C). Of note, none of these ICR-me QTLs were located on the same chromosome (Chr) as their putative target ICRs, indicating that each of the identified QTL regions functions in *trans*. Two ICR-me QTLs—located on Chr4 and Chr17—are associated with multiple ICRs, with the Chr4 QTL showing the strongest association with ICRs from the *Grb10*, *Mest*, *Plagl1*, and *Zsr1* loci and the Chr17 QTL associating strongest with ICRs at the *H19*, *Gtl2* promoter, and *Zbdf2*_pat loci (Figure 2C). Several additional ICRs and non-imprinted genes showed elevated logarithm of odds (LOD) scores at these QTLs, suggesting that these regions harbor variants controlling the degree of DNA hypomethylation across multiple genomic target sites (Figure 2C).

The Chr4 QTL region (Chr4: 144,920,230-151,337,450) contains a large cluster of genes encoding KRAB zinc-finger proteins (KRAB-ZFPs) (Figure 2D), which are rapidly evolving genes that play essential roles in silencing foreign DNA elements such as retrotransposons and endogenous retroviruses. Several prior genetic mapping studies have implicated this genomic region in regulating DNA methylation, including as a modulator of transgene silencing (Engler et al., 1991) and of variably methylated intracisternal A particle elements that can act as epi-alleles in mice (Bertozzi et al., 2020; Wolf et al., 2020). In addition, gene expression and chromatin accessibility QTL (caQTL) mapping in nPSCs from DO mice identified this region as a *trans*-eQTL/caQTL hotspot linked to changes in gene expression (115 affected genes) and chromatin accessibility (577 affected peaks) (Skelly et al., 2020). In contrast, to our knowledge, the region of Chr17 QTL (Chr17: 31,353,698-33,102,392) has not yet been implicated in regulating nPSC transcription or biology. Analysis of the Chr17 QTL suggested several candidate genes that could contribute to the regulation of DNA methylation, including a cluster of genes encoding KRAB-ZFP proteins (*Zfp871*, *Zfp870*, *Zfp799*, *Zfp763*, and *Zfp472*), the transcriptional co-activator *Brd4*, and *Wiz*, a known interaction partner of the repressive histone methyltransferases EHMT1 and EHMT2 (also known as GLP and G9a) (Figure 2E).

Of note, allelic effect analysis showed different contributions of specific DO founder strain haplotypes at the Chr4 and the Chr17 QTL (Figures 2F and 2G). In particular, B6J and 129 had opposite effects on DNA methylation changes mediated by the Chr17 QTL (Figure 2G), raising the possibility that this region might be involved in establishing the strain-specific DNA methylation stability observed in pure background nPSCs from these two strains. Among the genes found in the Chr17 QTL critical interval,

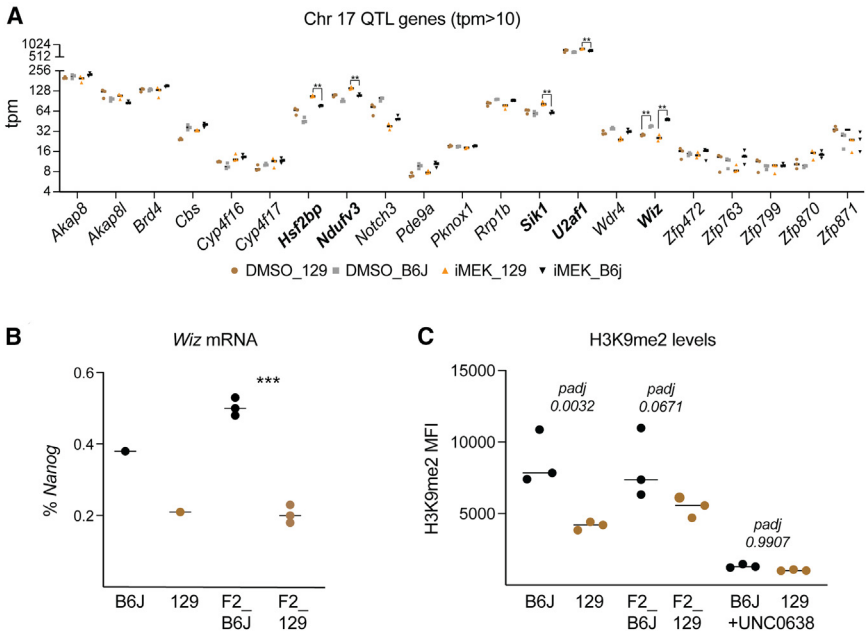

Figure 3. Characterization of the Chr17 QTL

(A) RNA-seq expression levels of all genes encoded by the Chr17 QTL with tpm > 10 in either B6J or 129 mESCs. $^{**}q < 0.01$ with multiple t tests and Benjamini, Krieger, and Yekutieli corrections.

(B) *Wiz* mRNA levels as determined by qPCR in pure background mESCs and F2 mESCs that are homozygous for either the B6J (F2_B6J) or the 129 (F2_129) allele of the Chr17 QTL (n = 3 clonal lines for each genotype). Statistics with unpaired t test.

(C) H3K9me2 levels as determined by intracellular flow cytometry in pure background mESCs and F2 mESCs that are homozygous for either the B6J (F2_B6J) or the 129 (F2_129) allele of the Chr17 QTL and pure background mESCs exposed to the EHMT1/2 inhibitor UNC0638 (n = 3 clonal lines for each genotype). Statistics with one-way ANOVA.

transcriptomic analysis in B6J and 129 mESCs revealed that *Wiz* is significantly higher expressed in B6J nPSCs (Figure 3A). Similarly, we found that F2 (129; B6J) mESCs (Swanzey et al., 2020) homozygous for the B6J allele of the Chr17 QTL ($Chr17^{B6J/B6J}$) (Figure S3A) expressed higher levels of *Wiz* mRNA levels than F2 mESCs with the 129 allele ($Chr17^{129/129}$) (Figure 3B). *Wiz* was initially identified in an ENU screen for genes that modulate the rate of stochastic epigenetic silencing of an integrated reporter transgene (Daxinger et al., 2013). The EHMT1/2 complex, which catalyzes the repressive H3K9me2 mark and interacts directly with WIZ (Simon et al., 2015), has been linked to the regulation of DNA methylation at several ICRs (Zhang et al., 2016). $Chr17^{B6J/B6J}$ F2 mESCs also exhibited higher H3K9me2 levels than $Chr17^{129/129}$ F2 mESCs. Unlike inbred B6J mESCs, this difference did not reach statistical significance (Figure 3C). Of note, inhibition of the enzymatic activity of EHMT1/2 greatly reduced H3K9me2 levels in both 129 and B6J mESCs, documenting the importance of these histone methyltransferases in both backgrounds (Figures 3C and S3B). These observations suggest that the genotype of the Chr17 QTL directly controls *Wiz* expression levels in mESCs. At the same time, additional genetic factors that distinguish B6J and 129 mESCs influence cell type-specific H3K9me2 levels.

Interestingly, the *Wiz* locus contains a B6J-specific structural variant (ETn-ERV element insertion) (Baust et al., 2002), which could modulate *Wiz* expression. This is consistent with recent data from DO nPSCs that indicate that ETn-ERV element insertions are associated with local changes in chromatin accessibility (Ferraj et al., 2023). Further investigation will be needed to confirm the specific sequence variant(s) that contribute to variable *Wiz* expression levels in mESCs and the potential role of WIZ in protecting ICR methylation stability.

DISCUSSION

The susceptibility of imprinted genes for dysregulation in mouse and human pluripotent cells and the associated risks have been well established. More recently, efforts to establish naive pluripotency in human cells have drawn additional attention to the issue of pathological DNA hypomethylation in these cells (Bar and Benvenisty, 2019). Our results with inbred and genetically diverse nPSCs demonstrate that genetic background contributes significantly to variation in susceptibility to aberrant DNA hypomethylation during establishment and maintenance of naive pluripotency downstream of inhibition of MAPK signaling. The consistent changes in ERK phosphorylation and DNMT3A levels suggest that B6J and 129 mESCs are equally sensitive to the direct changes caused by iMEK. However, the DNA methylation stability is markedly different in these cells. Based on QTL mapping conducted in DO nPSCs, we propose that genetic variants modulating the activity of specific *trans*-acting factors—including KRAB-ZFPs and candidate co-factors such as WIZ—represent critical variables contributing to epigenetic instability in nPSCs. Of note, while KRAB-ZFPs undergo rapid evolution, ZFP57 and ZFP445 have been reported to protect ICRs from demethylation in both mice and humans (Takahashi et al., 2019; Juan and

Bartolomei, 2019), raising the possibility that variants in these proteins could affect epigenome stability in nPSCs from both species. Prior eQTL data from mouse nPSCs identified a link between KRAB-ZFPs within the Chr4 KRAB-ZFP cluster and *Wiz* expression (Skelly et al., 2020). A larger scale QTL mapping study will be necessary to parse further the relationship between these two regions and their effects on DNA methylation.

The impact of genetic variation on imprint stability in cultured pluripotent cells has several ramifications. First, cell line- and locus-specific vulnerabilities complicate the identification of a universal media composition that can stabilize imprints across different cell lines. This is documented by the background-specific requirements of B6J and 129 nPSCs, with B6J nPSCs better tolerating de-methylating agents such as iMEK and AA and 129 preserving imprints in serum-based culture conditions. Second, it may be possible to predict imprint stability in specific culture conditions based on the genetic variants in a given nPSC line. Third, the targeted re-engineering of specific variants could stabilize imprints in otherwise epigenetically unstable PSCs. In addition to these practical considerations, the systematic identification and characterization of variants that impact imprint stability in nPSCs might help to unravel the complex regulatory networks governing DNA methylation stability, with implications for a wide range of physiological and pathological processes.

Limitations of the study

Given the relatively small sample size of the current study (n = 73 DO lines), we could only identify QTLs with relatively large effect sizes. In addition, we cannot comprehensively map QTLs that contribute to variation in DNA methylation since we used a targeted capture panel for a pre-defined set of genomic regions. Genome-wide DNA methylation profiling on a larger set of DO nPSC lines would likely identify additional QTLs and further clarify the relationship between genetic variation and DNA methylation stability in nPSCs. Since probe design and read mapping were performed using the C57BL/6 reference genome, it is possible that genomic regions with highly divergent haplotypes among the DO strains might not be quantified accurately. However, based on the assessment of the targeted capture approach and downstream read mapping pipeline, this issue should not impact the QTLs mapped in the current study.

METHODS

Cell culture

MEF cultures were established from late midgestation embryos and maintained in MEF media. Reprogramming was achieved with a dox-inducible polycistronic STEMCCA lentivirus encoding OCT4, KLF4, SOX2, and MYC (Sommer et al., 2009) using an enhanced media composition (Vidal et al., 2014). After day 7, cultures were continued in ESC medium supplemented with AA until P3 and in base ESC medium until P15. ESC lines from inbred mouse strains were derived as previously described (Czechanski et al., 2014). Mouse strain maintenance, crosses and tissue isolation were performed according to protocols approved by the Institutional Animal Care and Use Committees of Weill Cornell Medical College. ESC lines from DO mice were generated via a pooled IVF procedure (Glenn et al., 2024). See Table S1 for details on all cell lines.

DNA methylation analysis by targeted capture

A Custom Twist Methylome Panel (Twist Bioscience) was designed to perform targeted enrichment for genomic regions chosen based on their known functions as ICRs (Dahlet et al., 2020; Swanzey et al., 2020) or association with germline (Mochizuki et al., 2021), mouse pre-implantation (Hu et al., 2020) and post-implantation development (Dahlet et al., 2020) or aging (Meer et al., 2018; Stubbs et al., 2017), and cancer (Brady et al., 2021) (Table S2). DO ESCs were at passages 4–5 in mESC+2i media for 2–4 days, harvested using collagenase IV (500 U/mL) and shipped to SAMPLED (Piscataway, NJ) for processing using Twist NGS Methylation Detection Workflow.

RNA isolation and analysis

Total RNA from cells was extracted using TRIzol (Invitrogen 15596018) and purified using the RNA Clean and Concentrator kit (Zymo Research ZR1014). RNA quality and quantity were checked using a nanodrop. RNA-seq libraries were prepared using the TruSeq Stranded mRNA Library Prep Kit (Illumina# 20020595) and sequenced at PE 2X100 at the Genomics Core of Weill Cornell Medicine. Reverse transcription was performed using the iScript kit (Bio-Rad 1708841). qPCR was performed on cDNA samples with PowerUp SYBR green PCR master mix (Thermo Fisher A25778) and primers listed in Table S3.

Quantification and statistical analyses

Statistical analysis of flow cytometry and immunofluorescence data was done in PRISM 9 (GraphPad), with specific tests and corrections applied as indicated in the respective figure legends.

Additional experimental procedures and data analyses are detailed in the supplemental information.

RESOURCE AVAILABILITY

Lead contact

Stadtfeld M. (mas4011@med.cornell.edu).

Materials availability

Cell lines generated in this study are available upon request from the lead contact. Diversity Outbred mESC lines are described in the study by Glenn et al. (2024) and can be requested from Thomas Vierbuchen (vierbuct@mskcc.org).

Data and code availability

Source data are available in the Gene Expression Omnibus under the accession numbers NCBI GEO: GSE268906 (EM-seq) and NCBI GEO: GSE267262 (RNA-seq). FAIR data management principles (Wilkinson et al., 2016) were considered when preparing public datasets.

ACKNOWLEDGMENTS

We thank Subhashini Madhuranath for help with WB and Laurianne Scourzic for providing reprogramming virus. We are grateful to all M.S., T.V., and E.A. lab members for their input on this project and feedback on this manuscript. M.S. was supported by grants from the NIH (R01GM145864), the Simons Foundation, the Tri-Institutional Stem Cell Initiative (Tri-SCI), and the Bohmfalk Charitable Trust. T.V. was supported by the Sloan Kettering Institute Josie Robertson Investigator Program, the Tri-Institutional Stem Cell Initiative (Tri-SCI), and the Sloan Kettering Institute Cancer Center Support Grant (NIH P30 CA008748). R.A.G. was supported via an NIH T32 training grant (T32 HD060600). J.G.M. received support from the NIH (R01GM145864, R01EB027918, R33HL151355, and R01 HL166983).

AUTHOR CONTRIBUTIONS

C.P. derived and characterized iPSCs from inbred mouse strains, isolated gDNA, and coordinated DNA methylation analysis by targeted bisulfite sequencing. R.A.G. led the effort to generate and characterize mESCs from DO mice, with assistance from S.S. and S.C.D. Y.F. performed *in vitro* fertilization and mESC derivation for Diversity Outbred mESC lines. Y.S. conducted QTL mapping. K.C. conducted WB and qPCR experiments and analyses and prepared samples for RNA-seq. K.K. conducted intracellular flow experiments. E.E.S. derived inbred mESCs. Y.Z. analyzed DNA methylation data. M.T. conducted TLC. E.A. supervised data analysis and contributed to conceiving the study. A.P. analyzed RNA-seq data. R.K. supervised bioinformatic analysis. J.G.M. supervised QTL mapping. M.S. and T.V. conceived the study, supervised the experiments, and wrote the manuscript with input from all authors.

DECLARATION OF INTERESTS

The authors declare no competing interests.

SUPPLEMENTAL INFORMATION

Supplemental information can be found online at https://doi.org/10.1016/j.stemcr.2025.102450.

Received: July 3, 2024
Revised: February 13, 2025
Accepted: February 13, 2025
Published: March 13, 2025

REFERENCES

Bar, S., and Benvenisty, N. (2019). Epigenetic aberrations in human pluripotent stem cells. EMBO J. *38*, e101033.

Baust, C., Baillie, G.J., and Mager, D.L. (2002). Insertional polymorphisms of ETn retrotransposons include a disruption of the wiz gene in C57BL/6 mice. Mamm. Genome *13*, 423–428.

Bayerl, J., Ayyash, M., Shani, T., Manor, Y.S., Gafni, O., Massarwa, R., Kalma, Y., Aguilera-Castrejon, A., Zerbib, M., Amir, H., et al. (2021). Principles of signaling pathway modulation for enhancing human naive pluripotency induction. Cell Stem Cell *28*, 1549–1565.

Bertozzi, T.M., Elmer, J.L., Macfarlan, T.S., and Ferguson-Smith, A.C. (2020). KRAB zinc finger protein diversification drives mammalian interindividual methylation variability. Proc. Natl. Acad. Sci. USA *117*, 31290–31300.

Blaschke, K., Ebata, K.T., Karimi, M.M., Zepeda-Martínez, J.A., Goyal, P., Mahapatra, S., Tam, A., Laird, D.J., Hirst, M., Rao, A., et al. (2013). Vitamin C induces Tet-dependent DNA demethylation and a blastocyst-like state in ES cells. Nature *500*, 222–226.

Bock, C., Kiskinis, E., Verstappen, G., Gu, H., Boulting, G., Smith, Z.D., Ziller, M., Croft, G.F., Amoroso, M.W., Oakley, D.H., et al. (2011). Reference Maps of human ES and iPS cell variation enable high-throughput characterization of pluripotent cell lines. Cell *144*, 439–452.

Brady, N.J., Bagadion, A.M., Singh, R., Conteduca, V., Van Emmenis, L., Arceci, E., Pakula, H., Carelli, R., Khani, F., Bakht, M., et al. (2021). Temporal evolution of cellular heterogeneity during the progression to advanced AR-negative prostate cancer. Nat. Commun. *12*, 3372.

Byers, C., Spruce, C., Fortin, H.J., Hartig, E.I., Czechanski, A., Munger, S.C., Reinholdt, L.G., Skelly, D.A., and Baker, C.L. (2022). Genetic control of the pluripotency epigenome determines differentiation bias in mouse embryonic stem cells. EMBO J. *41*, e109445.

Choi, J., Huebner, A.J., Clement, K., Walsh, R.M., Savol, A., Lin, K., Gu, H., Di Stefano, B., Brumbaugh, J., Kim, S.Y., et al. (2017). Prolonged Mek1/2 suppression impairs the developmental potential of embryonic stem cells. Nature *548*, 219–223.

Claxton, M., Pulix, M., Seah, M.K.Y., Bernardo, R., Zhou, P., Aljuraysi, S., Liloglou, T., Arnaud, P., Kelsey, G., Messerschmidt, D.M., and Plagge, A. (2022). Variable allelic expression of imprinted genes at the Peg13, Trappc9, Ago2 cluster in single neural cells. Front. Cell Dev. Biol. *10*, 1022422.

Czechanski, A., Byers, C., Greenstein, I., Schrode, N., Donahue, L.R., Hadjantonakis, A.K., and Reinholdt, L.G. (2014). Derivation and characterization of mouse embryonic stem cells from permissive and nonpermissive strains. Nat. Protoc. *9*, 559–574.

Dahlet, T., Argüeso Lleida, A., Al Adhami, H., Dumas, M., Bender, A., Ngondo, R.P., Tanguy, M., Vallet, J., Auclair, G., Bardet, A.F.,

and Weber, M. (2020). Genome-wide analysis in the mouse embryo reveals the importance of DNA methylation for transcription integrity. Nat. Commun. *11*, 3153.

Daxinger, L., Harten, S.K., Oey, H., Epp, T., Isbel, L., Huang, E., Whitelaw, N., Apedaile, A., Sorolla, A., Yong, J., et al. (2013). An ENU mutagenesis screen identifies novel and known genes involved in epigenetic processes in the mouse. Genome Biol. *14*, R96.

Duffié, R., Ajjan, S., Greenberg, M.V., Zamudio, N., Escamilla del Arenal, M., Iranzo, J., Okamoto, I., Barbaux, S., Fauque, P., and Bourc'his, D. (2014). The Gpr1/Zdbf2 locus provides new paradigms for transient and dynamic genomic imprinting in mammals. Gene Dev. *28*, 463–478.

Engler, P., Haasch, D., Pinkert, C.A., Doglio, L., Glymour, M., Brinster, R., and Storb, U. (1991). A strain-specific modifier on mouse chromosome 4 controls the methylation of independent transgene loci. Cell *65*, 939–947.

Ferguson-Smith, A.C., and Bourc'his, D. (2018). The discovery and importance of genomic imprinting. Elife *7*, e42368.

Ferraj, A., Audano, P.A., Balachandran, P., Czechanski, A., Flores, J.I., Radecki, A.A., Mosur, V., Gordon, D.S., Walawalkar, I.A., Eichler, E.E., et al. (2023). Resolution of structural variation in diverse mouse genomes reveals chromatin remodeling due to transposable elements. Cell Genom. *3*, 100291.

Gatti, D.M., Svenson, K.L., Shabalin, A., Wu, L.Y., Valdar, W., Simecek, P., Goodwin, N., Cheng, R., Pomp, D., Palmer, A., et al. (2014). Quantitative trait locus mapping methods for diversity outbred mice. G3 (Bethesda) *4*, 1623–1633.

Glenn, R.A., Do, S.C., Guruvayurappan, K., Corrigan, E.K., Santini, L., Medina-Cano, D., Singer, S., Cho, H., Liu, J., Broman, K., et al. (2024). A Pluripotent Stem Cell Platform for in Vitro Systems Genetics Studies of Mouse Development. Preprint at bioRxiv. https://doi.org/10.1101/2024.06.06.597758.

Habibi, E., Brinkman, A.B., Arand, J., Kroeze, L.I., Kerstens, H.H.D., Matarese, F., Lepikhov, K., Gut, M., Brun-Heath, I., Hubner, N.C., et al. (2013). Whole-genome bisulfite sequencing of two distinct interconvertible DNA methylomes of mouse embryonic stem cells. Cell Stem Cell *13*, 360–369.

Hu, Z., Tan, D.E.K., Chia, G., Tan, H., Leong, H.F., Chen, B.J., Lau, M.S., Tan, K.Y.S., Bi, X., Yang, D., et al. (2020). Maternal factor NELFA drives a 2C-like state in mouse embryonic stem cells. Nat. Cell Biol. *22*, 175–186.

Humpherys, D., Eggan, K., Akutsu, H., Hochedlinger, K., Rideout, W.M., Biniszkiewicz, D., Yanagimachi, R., and Jaenisch, R. (2001). Epigenetic instability in ES cells and cloned mice. Science *293*, 95–97.

Johannesson, B., Sagi, I., Gore, A., Paull, D., Yamada, M., Golan-Lev, T., Li, Z., LeDuc, C., Shen, Y., Stern, S., et al. (2014). Comparable frequencies of coding mutations and loss of imprinting in human pluripotent cells derived by nuclear transfer and defined factors. Cell Stem Cell *15*, 634–642.

Juan, A.M., and Bartolomei, M.S. (2019). Evolving imprinting control regions: KRAB zinc fingers hold the key. Genes Dev. *33*, 1–3.

Lee, J., Matsuzawa, A., Shiura, H., Sutani, A., and Ishino, F. (2018). Preferable *in vitro* condition for maintaining faithful DNA methylation imprinting in mouse embryonic stem cells. Genes Cells *23*, 146–160.

Mani, S., and Mainigi, M. (2018). Embryo Culture Conditions and the Epigenome. Semin. Reprod. Med. *36*, 211–220.

Meer, M.V., Podolskiy, D.I., Tyshkovskiy, A., and Gladyshev, V.N. (2018). A whole lifespan mouse multi-tissue DNA methylation clock. Elife *7*, e40675.

Mochizuki, K., Sharif, J., Shirane, K., Uranishi, K., Bogutz, A.B., Janssen, S.M., Suzuki, A., Okuda, A., Koseki, H., and Lorincz, M.C. (2021). Repression of germline genes by PRC1.6 and SETDB1 in the early embryo precedes DNA methylation-mediated silencing. Nat. Commun. *12*, 7020.

Ortmann, D., Brown, S., Czechanski, A., Aydin, S., Muraro, D., Huang, Y., Tomaz, R.A., Osnato, A., Canu, G., Wesley, B.T., et al. (2020). Naive Pluripotent Stem Cells Exhibit Phenotypic Variability that Is Driven by Genetic Variation. Cell Stem Cell *27*, 470–481.e6.

Pastor, W.A., Chen, D., Liu, W., Kim, R., Sahakyan, A., Lukianchikov, A., Plath, K., Jacobsen, S.E., and Clark, A.T. (2016). Naive Human Pluripotent Cells Feature a Methylation Landscape Devoid of Blastocyst or Germline Memory. Cell Stem Cell *18*, 323–329.

Rebuzzini, P., Zuccotti, M., Redi, C.A., and Garagna, S. (2016). Achilles' heel of pluripotent stem cells: genetic, genomic and epigenetic variations during prolonged culture. Cell. Mol. Life Sci. *73*, 2453–2466.

Simon, J.M., Parker, J.S., Liu, F., Rothbart, S.B., Ait-Si-Ali, S., Strahl, B.D., Jin, J., Davis, I.J., Mosley, A.L., and Pattenden, S.G. (2015). A Role for Widely Interspaced Zinc Finger (WIZ) in Retention of the G9a Methyltransferase on Chromatin. J. Biol. Chem. *290*, 26088–26102.

Skelly, D.A., Czechanski, A., Byers, C., Aydin, S., Spruce, C., Olivier, C., Choi, K., Gatti, D.M., Raghupathy, N., Keele, G.R., et al. (2020). Mapping the Effects of Genetic Variation on Chromatin State and Gene Expression Reveals Loci That Control Ground State Pluripotency. Cell Stem Cell *27*, 459–469.e8.

Sommer, C.A., Stadtfeld, M., Murphy, G.J., Hochedlinger, K., Kotton, D.N., and Mostoslavsky, G. (2009). Induced pluripotent stem cell generation using a single lentiviral stem cell cassette. Stem Cell. *27*, 543–549.

Stubbs, T.M., Bonder, M.J., Stark, A.K., Krueger, F., BI Ageing Clock Team, von Meyenn, F., Stegle, O., and Reik, W. (2017). Multi-tissue DNA methylation age predictor in mouse. Genome Biol. *18*, 68.

Swanzey, E., McNamara, T.F., Apostolou, E., Tahiliani, M., and Stadtfeld, M. (2020). A Susceptibility Locus on Chromosome 13 Profoundly Impacts the Stability of Genomic Imprinting in Mouse Pluripotent Stem Cells. Cell Rep. *30*, 3597–3604.e3.

Swanzey, E., O'Connor, C., and Reinholdt, L.G. (2021). Mouse Genetic Reference Populations: Cellular Platforms for Integrative Systems Genetics. Trends Genet. *37*, 251–265.

Takahashi, N., Coluccio, A., Thorball, C.W., Planet, E., Shi, H., Offner, S., Turelli, P., Imbeault, M., Ferguson-Smith, A.C., and Trono, D. (2019). ZNF445 is a primary regulator of genomic imprinting. Genes Dev. *33*, 49–54.

Vidal, S.E., Amlani, B., Chen, T., Tsirigos, A., and Stadtfeld, M. (2014). Combinatorial modulation of signaling pathways reveals

cell-type-specific requirements for highly efficient and synchronous iPSC reprogramming. Stem Cell Rep. *3*, 574–584.

Wilkinson, M.D., Dumontier, M., Aalbersberg, I.J.J., Appleton, G., Axton, M., Baak, A., Blomberg, N., Boiten, J.W., da Silva Santos, L.B., Bourne, P.E., et al. (2016). The FAIR Guiding Principles for scientific data management and stewardship. Sci. Data *3*, 160018.

Wolf, G., de Iaco, A., Sun, M.A., Bruno, M., Tinkham, M., Hoang, D., Mitra, A., Ralls, S., Trono, D., and Macfarlan, T.S. (2020). KRAB-zinc finger protein gene expansion in response to active retrotransposons in the murine lineage. Elife *9*, e56337.

Yagi, M., Kishigami, S., Tanaka, A., Semi, K., Mizutani, E., Wakayama, S., Wakayama, T., Yamamoto, T., and Yamada, Y. (2017). Derivation of ground-state female ES cells maintaining gamete-derived DNA methylation. Nature *548*, 224–227.

Zhang, T., Termanis, A., Özkan, B., Bao, X.X., Culley, J., de Lima Alves, F., Rappsilber, J., Ramsahoye, B., and Stancheva, I. (2016). G9a/GLP Complex Maintains Imprinted DNA Methylation in Embryonic Stem Cells. Cell Rep. *15*, 77–85.

Zvetkova, I., Apedaile, A., Ramsahoye, B., Mermoud, J.E., Crompton, L.A., John, R., Feil, R., and Brockdorff, N. (2005). Global hypomethylation of the genome in XX embryonic stem cells. Nat. Genet. *37*, 1274–1279.